MATERIALS CHEMISTRY FRONTIERS

RESEARCH ARTICLE

View Article Online
View Journal

Cite this: DOI: 10.1039/d6qm00155f

One-pot postsynthetic linkage modification of imine covalent organic frameworks *via* iminium activation

Chonglu Wang,†[a] Tian Wang,†[a] Shuqi Jiang,†[a] Mengmeng Jia,[a] Yaqi Wei,[a] Yin-Shan Meng,[ac] Jiyun Hu*[b] and Tao Liu*[ac]

Received 26th February 2026,
Accepted 28th April 2026

DOI: 10.1039/d6qm00155f

rsc.li/frontiers-materials

Postsynthetic modification (PSM) of the linkages in covalent organic frameworks (COFs) is usually performed on isolated samples due to their incompatibility with the crystallization conditions. In this work, we report a one-pot PSM strategy that reduces imine-linked to amine-linked COFs *via* an iminium-activated process under acidic conditions. Using Hantzsch ester as a mild, chemoselective reductant, this method eliminates the need for isolating pristine COFs prior to transformation and shows better functional group tolerance compared to previous methods ($NaBH_4$ and HCOOH). The resulting amine-linked COFs retain high porosity and crystallinity. As a demonstration, a H_3PO_4-loaded amine-linked pyrene COF achieves a proton conductivity of 4.9×10^{-2} S cm^{-1} at 95 °C and 80% relative humidity with a low activation energy of 0.16 eV. This one-pot strategy offers a streamlined and general approach to accessing functionalized COFs.

Introduction

Guided by the principle of dynamic covalent chemistry,[1–4] chemists have successfully crystallized organic polymers, once thought impossible, into two- and three-dimensions held together entirely by strong covalent bonds.[5,6] These new materials, known as covalent organic frameworks (COFs), show great potential in gas storage/purification, catalysis, optoelectronics, and more, owing to their permanent porosity, ordered structure, and designable architecture.[7–10] Among various reactions developed for crystallizing COFs, the Schiff base condensation reaction stands out due to its rich library of linkers and the exceptional crystallinity of the resulting imine network.[11] Recently, there has been a surge of interest in postsynthetic modifications (PSMs) that convert and lock the C=N linkage, enhancing the stability and functionality of the framework.[12–14] Examples of successful PSMs include oxidation to amide,[15] reduction to amine,[16] and cyclization to heterocycles like oxazole,[17–19] thiazole,[17,20] oxadiazole,[21] and others.[22–24] PSMs have become an indispensable complementary method to access diverse linkages that are challenging to make *via de novo* synthesis. However, a key challenge associated with PSMs is the incompatibility between crystallization and transformation conditions, which necessitates the isolation and purification of COFs before the desired transformation, complicating the stepwise process. Furthermore, the specific conditions required for PSMs can potentially lead to partial or complete loss of crystallinity. Therefore, developing compatible conditions for both COF crystallization and subsequent PSMs would not only simplify the overall synthetic process in a one-pot manner but also crucially reduce the risk of crystallinity loss.

One-pot reactions, where several reaction sequences are conducted in a single reaction vessel, offer a powerful and green approach to synthetic organic chemistry.[25–27] This strategy minimizes chemical waste, saves energy and time, and simplifies practical aspects. However, the one-pot synthesis of COFs remains largely unexplored. To the best of our knowledge, only one report describes a one-pot Suzuki coupling followed by Schiff base condensation for imine COFs preparation.[28] Imine COFs are typically crystallized solvothermally with an acid catalyst, protic or metallic.[29–31] As a matter of fact, the primary amine-derived imines are basic, and they readily exist as iminium ions in an acidic solution.[32] The same phenomenon was observed on various imine COFs as well.[33–35] Iminiums are more electrophilic, up to 10 orders of magnitude, than the corresponding aldehydes or ketones.[36] This type of activation has triggered iminium catalysis, or described as "LUMO-lowering catalysis" by MacMillan and co-workers,[37] for various reactions such as cycloadditions,

[a] State Key Laboratory of Fine Chemicals, Frontier Science Center for Smart Materials, School of Chemical Engineering, Dalian University of Technology, No. 2 Linggong Road, Dalian 116024, China. E-mail: liutao@dlut.edu.cn
[b] Dongguan Key Laboratory of Interdisciplinary Science for Advanced Materials and Large-Scale Scientific Facilities, School of Physical Sciences, Great Bay University, Dongguan 523000, China. E-mail: hujiyun@gbu.edu.cn
[c] Liaoning Binhai Laboratory, Dalian 116023, China
† These authors contribute equally to this work.

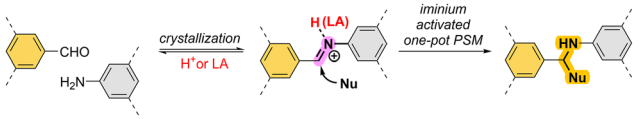

Fig. 1 Streamlined one-pot imine COF formation and subsequent PSM *via* an iminium-activated process (LA, Lewis acid).

nucleophilic additions, retro-aldol reactions, and so on.[32,38] In this context, imine COFs are inherently activated for PSMs under their acidic preparation conditions, yet overlooked in previous studies. Therefore, we propose a highly practicable one-pot PSM protocol for imine COFs that leverages the acidic synthetic conditions *via* an iminium-activated process (Fig. 1).

As a proof of concept, this work demonstrates the catalytic one-pot reduction of imine- to amine-linked COFs using Hantzsch ester, a biomimetic, inexpensive, stable, and safe reductant commonly employed in transfer hydrogenation reactions, including imines.[39–41] This protocol features high selectivity and broad COF scope. Amine-linked COFs have been shown to display superior catalytic performance and enhanced stability compared to their imine counterparts.[16,42–45] The amine linkage could also serve as a reactive handle for further functional group installation.[44,46,47] Current methods for converting imine- to amine-linked COFs rely on borohydride-based reagents, which suffer from limited selectivity and poor functional group tolerance.[16,48] Formic acid as an alternative reductant only works for metal nanoparticle-free COFs to avoid detrimental catalytic reduction that disrupts crystallinity.[47,49] While *in situ* reduction using bifunctional H_3PO_3 catalysts has been reported, it often results in limited crystallinity.[43] In this regard, a milder and more general method for the hydrogenation of imine COFs is highly desirable.

Results and discussion

Chemoselective reduction of 3D COF

We first studied the catalytic capability of acetic acid for the model imine reduction reaction between *N*-benzylideneaniline and diethyl 1,4-dihydro-2,6-dimethyl-3,5-pyridinedicarboxylate (HEH). In the presence of 3 equiv. of acetic acid, *ca.* 90% of *N*-benzylideneaniline was converted to *N*-benzylaniline with a stoichiometric amount of HEH at 70 °C for 6 hours in THF (Fig. S1 and S2). No reaction occurred without acetic acid, proving its critical role as a catalyst. Encouraged by the successful model reaction, we then started to apply the same chemistry to imine COFs. 3D pts COF, reticulated from 3,3′,5,5′-tetra(4-aminophenyl)-bimesitylene (BMTA) and hexa(4-formylphenyl)-benzene (HFB), was judiciously chosen to probe whether our proposed strategy would solve the aforementioned drawbacks for the following two reasons: (1) it is a substoichiometric network with one pair of unreacted reductant-sensitive formyl groups on HFB linker; (2) it has palladium contaminant inheriting from the Suzuki coupling produced linkers.[50]

To perform the one-pot reduction, 3 equiv. HEH (relative to amine groups) was introduced into the reaction vessel after

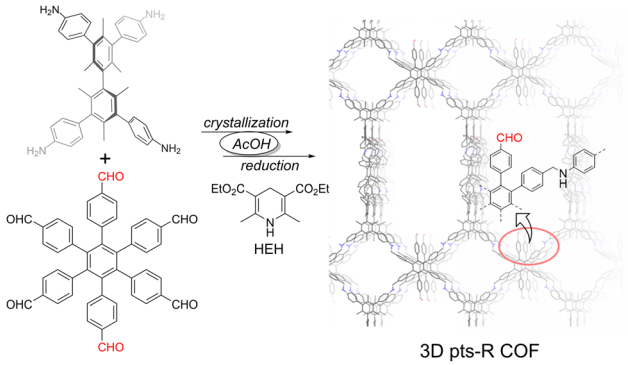

Scheme 1 One-pot PSM strategy for the synthesis of amine-linked 3D pts-R COF.

which 3D pts COF was formed in a mixture of dichlorobenzene/n-butanol/6 M acetic acid (Scheme 1). The mixture was heated at 120 °C for 24 h. The reduction using $NaBH_4$ and HCOOH was also conducted for comparisons (see SI for details). Multiple spectroscopic techniques confirmed the successful reduction of C═N to C–N linkage with HEH as well as $NaBH_4$ and HCOOH. FT-IR spectra show the absence of the C═N vibration band at 1624 cm^{-1} and the presence of C–N vibration at 1247 cm^{-1} for 3D pts-R COF in all three cases (R stands for reduced, footnote indicates the reductant, Fig. 2a). Meanwhile, the strong vibration band at 1702 cm^{-1} and the absence of OH vibration confirm the survival of formyl groups when HEH and HCOOH were used. However, in the case of $NaBH_4$, complete reduction of formyl to alcohol occurred, judging from the disappearance of the carbonyl vibration band and the presence of the OH vibration band at 3370 cm^{-1}. Solid-state cross-polarization magic angle spinning (CP/MAS) ^{13}C NMR spectroscopy corroborates the FT-IR results. The appearance of secondary amine carbon at 48.5 ppm and the vanished imine carbon at 158.4 ppm confirm full reduction of imine bonds for all three reduced COFs (Fig. 2b). The absence of the aldehyde carbon peak and the presence of a peak at 64.3 ppm ascribed to the CH_2OH group for pts-R_{NaBH4}, certify the non-selective reduction with $NaBH_4$. In contrast, no aldehyde reduction was observed for pts-R_{HEH} and pts-R_{HCOOH}. X-ray photoelectron spectroscopy (XPS) study shows the N 1s binding energy shifts from 398.4 eV for 3D pts COF to higher energy at 399.0 eV for 3D pts-R COF, while the O 1s binding energy does not change in the case of HEH and HCOOH being used (Fig. 2c). The reduction of formyl to alcohol with $NaBH_4$ is also evident from the shifted O 1s binding energy from 531.6 to 532.2 eV. All these results demonstrate the capability of HEH to exert a quantitative and selective reduction of imine into amine linkages. The crystallinity of 3D pts-R was examined by powder X-ray diffraction (PXRD) measurements. Interestingly, only pts-R_{HEH} showed a diffraction pattern similar to that of the parent imine COF (Fig. 2d). pts-R_{HCOOH} and pts-R_{NaBH4} are amorphous, likely resulting from the non-selective reduction process.[47] The presence of Pd nanoparticles in pst-R is evident in the transmission electron microscope (TEM) images (Fig. S3). Inductively coupled plasma-mass spectrometry (ICP-MS) reveals that the Pd content in 3D pts COF is 0.064%. The permanent porosity of 3D

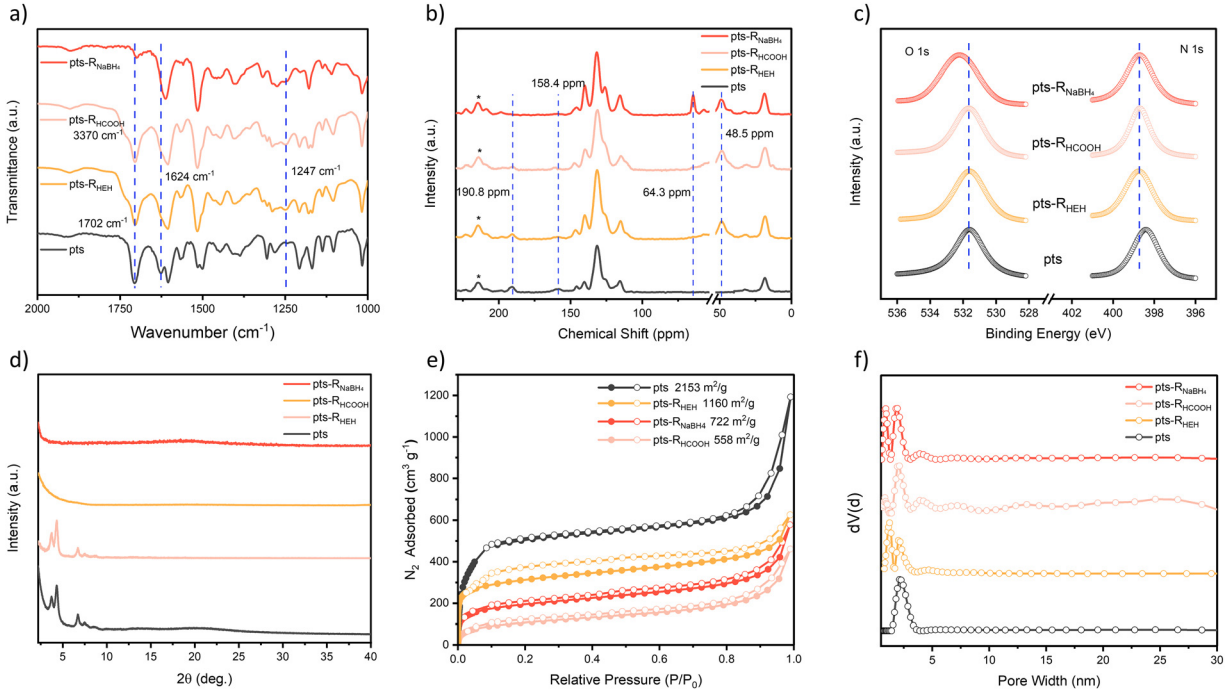

Fig. 2 FT-IR spectra (a), solid-state ^{13}C NMR spectra (b), N 1s XPS spectra (c), PXRD spectra (d), 77 K N_2 isotherms (e), and pore size distribution profiles (f) of 3D pts and pts-R COFs. Spinning sidebands are labelled with an asterisk in NMR spectra. To avoid the interference of spinning sidebands, NMR data of 0–60 ppm and 60–250 ppm were acquired at a spinning rate of 10 and 12.5 kHz, respectively.

pts-R was assessed by N_2 sorption experiments at 77 K (Fig. 2e). The BET surface areas were calculated to be 1160, 722, and 558 $m^2\ g^{-1}$ for pts-R_{HEH}, pts-R_{HCOOH}, and pts-R_{NaBH4}, respectively, lower than that of the parent imine COF (2153 $m^2\ g^{-1}$). It should be noted that pts-R_{HEH} shows a more pronounced hysteresis in its N_2 isotherm than R_{HCOOH} and pts-R_{NaBH4}. This is possibly from an enhanced framework-adsorbate interaction in the ordered flexible amine-linked structure. The pore size distribution of 3D pts-R was calculated based on the quenched solid-state density functional theory method. 3D pts-R shows a narrow pore-size distribution centered at 2.1 nm (Fig. 2f). All the reduced COFs show two major pores centered at 1.2 nm and 2.1 nm. The smaller pore likely results from the framework collapse due to the flexible C–N linkages. We measured the CO_2 adsorption properties of the reduced pts COFs, considering that the CHO group is reported to enhance CO_2 adsorption in addition to the more basic amine linkage.[51] The adsorption capacity of pts, pts-R_{HEH}, pts-R_{NaBH4}, and pts-R_{HCOOH} COF is measured to be 32.9, 31.5, 25.1, and 23.0 $cm^3\ g^{-1}$, respectively (298 K, 1 atm, Fig. S4). Despite much reduced surface areas compared to the pristine imine COF (1160 vs 2153 $m^2\ g^{-1}$), pts-R_{HEH} has a comparable CO_2 adsorption capacity to that of pts COF. In contrast, pts-R_{NaBH4} and pts-R_{HCOOH} show much lower capacity, highlighting the importance of crystallinity and aldehyde groups. Scanning electron microscopy (SEM) analysis shows that the reduction does not change morphology and particle size (Fig. S5). Our protocol thus represents a chemo-selective linkage transformation method, especially useful where polar formyl groups are needed as preferred functional groups.[51,52] Moreover, a detailed comparison of different reduction methods was summarized in Table S1. The HEH method requires less reagent consumption with comparative yields compared to other methods at a moderate cost. However, the reduction with HEH generates bulky pyridine-derived byproducts, resulting in a much lower atom economy than HCOOH and $NaBH_4$. Nevertheless, HEH is a far more convenient and safer reductant than both formic acid (corrosive, fuming liquid) and sodium borohydride (moisture-sensitive, flammable gas hazard), requiring no special inert atmosphere, corrosion-resistant equipment, or quenching protocols. Due to the relatively large molecular size of HEH (*ca.* 1.2 × 0.8 nm), COFs with small pore sizes are not suitable substrates. For instance, our attempt to reduce the imine linkages in COF-303 (pore size 0.8 nm) to amine linkages using HEH was unsuccessful (Fig. S6).

Catalytic reduction with Lewis acids

Lewis acids have been proven to be superior catalysts to commonly used acetic acid for synthesizing imine COFs in some cases.[30,31] Hexagonal 2D TAPB-DMTA COF, which could be crystallized with various Lewis acids, including $Sc(OTf)_3$,[30] $Fe(NO_3)_3{\cdot}9H_2O$,[53] and SbI_3,[54] besides acetic acid, was chosen to test the generality of the one-pot reduction procedure (Fig. 3a). Successful reduction to the amine-linked TAPB-DMTA-R COF was achieved for all tested catalysts as evidenced by FT-IR analysis (Fig. 3b). All the reduced samples display similar spectra featuring a disappeared C═N stretching band at 1616 cm^{-1} and an emerged C–N stretching band at 1260 cm^{-1}. Additionally, the increased N 1s binding energy (Fig. 3c) and presence of the carbon of secondary amine signal at 44.4 ppm in the CP/MAS ^{13}C NMR spectrum corroborate the FT-IR results (Fig. 3d). However,

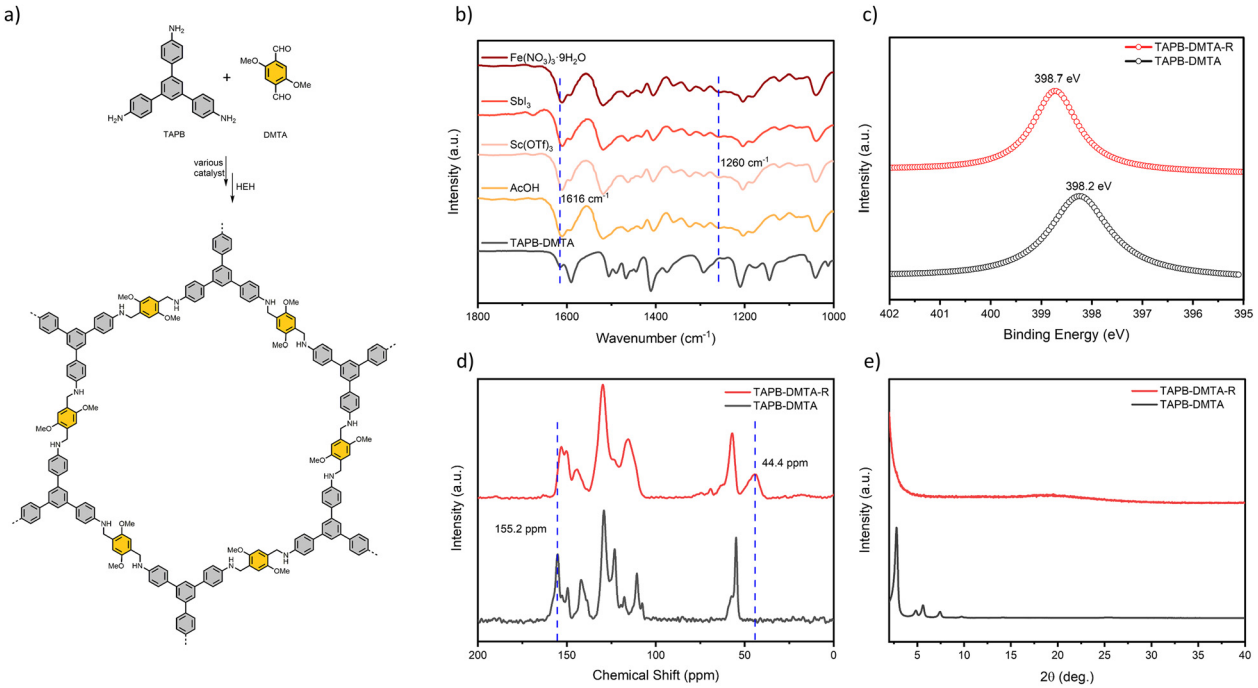

Fig. 3 (a) Synthetic scheme of TAPB-DMTA-R COF. (b) FT-IR spectra of TAPB-DMTA-R COF synthesized with different catalysts. Comparison of (c) N 1s XPS spectra, (d) solid-state ^{13}C NMR spectra, and (e) PXRD spectra of TAPB-DMTA and TAPB-DMTA-R COF.

PXRD analysis shows that TAPB-DMTA-R COF is amorphous (Fig. 3e), despite various mild activation procedures being used (solvent exchange with low surface tension solvents like hexane, diethyl ether, and $scCO_2$).[55] This is in line with the observed lower framework stability resulting from the high flexibility of the secondary amine bond.[22,47] To rule out the possibility of crystallinity damage induced by our PSM protocol, a partial reduction of TAPB-DMTA COF with a reduced amount of HEH was performed. In this case, a crystalline COF was obtained (Fig. S7–S10), supporting that the crystallinity loss of fully reduced TAPB-DMTA-R COF results from the framework's inherent flexibility rather than the reduction method. SEM analysis reveals that the reduction did not alter the morphology under these conditions (Fig. S11 and S12).

Synthesis of stable 2D amine-linked COF for proton conduction

After demonstrating the generality of the proposed one-pot reduction method, a stable amine-linked 2D COF was prepared against pore collapse using pyrene linkers (Fig. 4a). Py-Py COF condensed from 1,3,6,8-tetrakis(4-aminophenyl)pyrene (TAPPy) and 1,3,6,8-tetrakis(4-formylphenyl)pyrene (TFPPy) was crystallized in a mixture solvent of mesitylene/dioxane/DMA first.[56] Then 3 equiv. HEH was introduced, and the mixture was heated at 120 °C for 24 h (see SI for details). Multiple spectroscopic techniques confirmed the successful reduction of the C═N bond to a C–N linkage. FT-IR spectra show the absence of the C═N vibration band at 1621 cm^{-1} and the presence of the C–N vibration at 1253 cm^{-1} for Py-Py-R COF (Fig. S13a). Solid-state CP/MAS ^{13}C NMR spectroscopy reveals a new signal at 49.4 ppm ascribed to the carbon of secondary amine linkage (Fig. S13b), while no residual signal for the imine carbon at 156.2 ppm is present. XPS study shows the N 1s binding energy shifts from 398.2 eV for Py-Py COF to higher energy at 398.6 eV for Py-Py-R COF (Fig. S13c). All these results are consistent with a quantitative reduction of imine into amine linkages. The crystallinity of Py-Py-R was examined by powder X-ray diffraction (PXRD) measurements. The PXRD pattern of Py-Py-R is similar to that of the parent imine COF, showing a prominent diffraction peak at $2\theta = 2.60°$, along with other minor peaks at 5.07, 7.19, 10.19, 15.31, and 23.41° respectively (Fig. 4b). The permanent porosity of Py-Py-R was assessed by N_2 sorption experiments at 77 K (Fig. 4c). The BET surface areas were calculated to be 718 $m^2\ g^{-1}$, slightly lower than that of the parent imine COF (1109 $m^2\ g^{-1}$), and the pore volume is 0.61 $cm^3\ g^{-1}$. The pore size distribution of Py-Py-R was calculated based on the quenched solid-state density functional theory method, showing a narrow pore-size distribution centered at 1.46 and 2.36 nm (Fig. 4c). SEM and TEM analysis show that the reduction does not change the morphology and particle size of Py-Py-R COF (Fig. S14 and S15).

The saturated C–N linkage provides increased chemical stability and stronger interactions with acids, which render Py-Py-R a potential proton conduction material candidate when loaded with acids.[57,58] We prepared H_3PO_4-loaded Py-Py-R composites (H_3PO_4@Py-Py-R) *via* the impregnation method (see SI for details). FT-IR spectrum of H_3PO_4@Py-Py-R shows new bands at 2910, 1155, 1000, and 490 cm^{-1}, assigned to the O–H vibration, asymmetric P–O vibration, symmetric P–O vibration, and O–P–O bending modes, respectively, indicating successful H_3PO_4 loading (Fig. 4d).[59,60] The theoretical maximum phosphoric acid loading capacity of Py-Py-R estimated from its pore volume is *ca.*

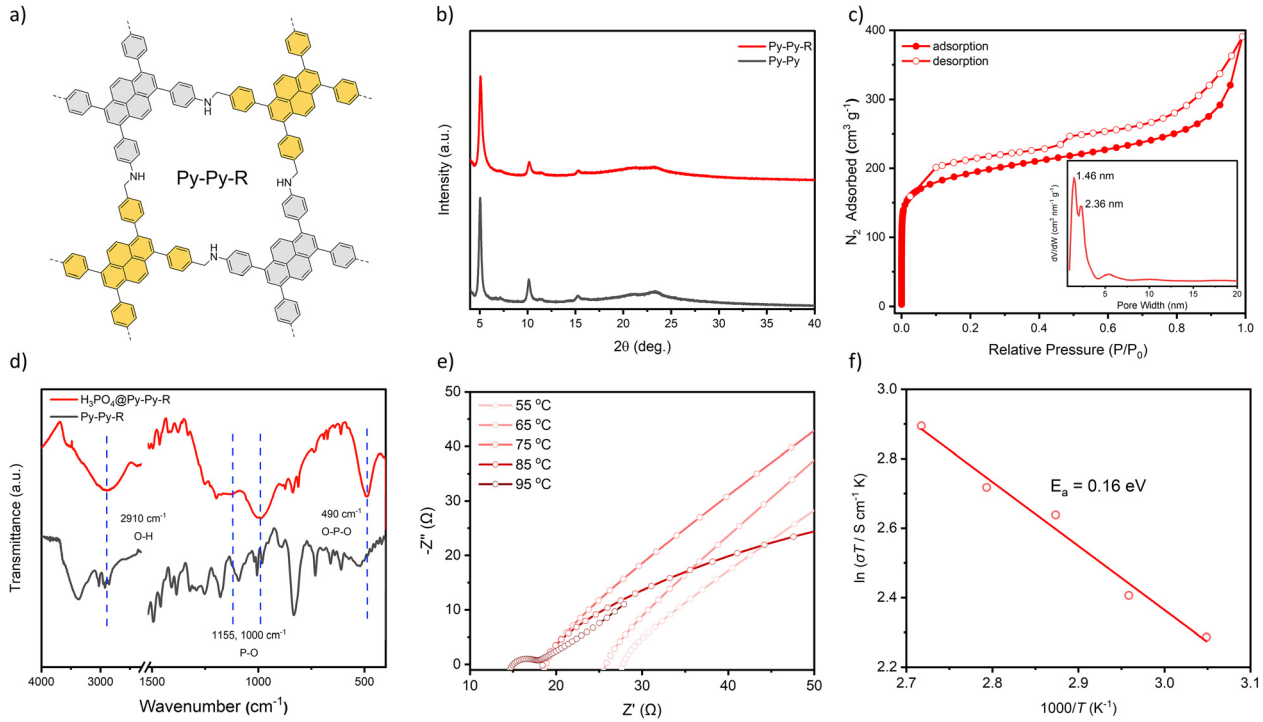

Fig. 4 (a) Chemical structure of Py-Py-R COF. (b) PXRD patterns of Py-Py and Py-Py-R. (c) 77 K N_2 isotherm of Py-Py-R (inset shows the pore size distribution profile). (d) Comparison of the FT-IR spectra of H_3PO_4@Py-Py-R and Py-Py-R. (e) Nyquist plots of H_3PO_4@Py-Py-R at various temperatures with 80% RH. (f) Arrhenius plot of H_3PO_4@Py-Py-R at 80% RH.

110 wt%. According to the increased mass amount, the H_3PO_4 loading of H_3PO_4@Py-Py-R was calculated to be 100 wt%, close to the theoretical maximum. Then, H_3PO_4@Py-Py-R powder was pressed into cylindrical pellets with a diameter of 6.0 mm and a thickness of around 1.0 mm for proton conduction tests using electrochemical impedance spectroscopy (EIS). As shown in Fig. 4e, the Nyquist plots of H_3PO_4@Py-Py-R at 80% relative humidity (RH) exhibit typical ionic conduction characteristics, confirming its proton transport capability. When the temperature increases from 45 °C to 95 °C, the impedance of H_3PO_4@Py-Py-R steadily decreases. The corresponding proton conductivity increases from 3.0×10^{-2} S cm^{-1} at 55 °C to 4.9×10^{-2} S cm^{-1} at 95 °C (Fig. S16). This performance is comparable to those of the reported best-performing COF materials under similar conditions (Table S2).[61,62] The activation energy (E_a) fitted from the Arrhenius plot is 0.16 eV (Fig. 4f). This value is substantially lower than the typical threshold for the vehicle mechanism (>0.4 eV), indicating that proton transport occurs predominantly *via* concerted hopping along the hydrogen-bonded network (the Grotthuss mechanism). These results demonstrate that amine-linked COFs could be potential proton conduction materials.

Conclusions

In summary, we reported here a one-pot PSM procedure to reduce imine to amine-linked COFs *via* iminium activation using Hantzsch ester as the reductant. The procedure is not only operationally simple but also circumvents various drawbacks of the previous methods, such as poor functional group tolerance and sensitivity to metal impurities. Besides, both 2D and 3D COFs can be successfully reduced. Moreover, this iminium activation strategy is not only effective in systems catalyzed by Brønsted acids, but likewise in those employing Lewis acids. We believe the presented iminium activation concept would expand the applications of amine-linked COFs and inspire new functionalization methods for imine-based materials beyond COFs.

Author contributions

C. Wang: data curation, formal analysis, methodology. T. Wang: data curation, formal analysis, methodology. S. Jiang: data curation, formal analysis, methodology. M. Jia: data curation. Y. Wei: data curation. Y.-S. Meng: writing-review & editing, project administration, supervision, funding acquisition. J. Hu: writing-review & editing, project administration, supervision, funding acquisition. T. Liu: writing-review & editing, project administration, supervision, funding acquisition.

Conflicts of interest

There are no conflicts to declare.

Data availability

The data supporting this article have been included as part of the supplementary information (SI). Supplementary information:

Fig. S1–S16 and further experimental details. See DOI: https://doi.org/10.1039/d6qm00155f.

Acknowledgements

This work was supported by the National Natural Science Foundation of China (Grants 22401035, 22025101, 22222103, 22173015), the Fundamental Research Funds for the Central Universities (DUT22LAB606), Liaoning Binhai Laboratory (LBLE-2023-02), and "Excellence Co-innovation Program" International Exchange Fund Project (DUTIO-ZG-202505), Guangdong Basic and Applied Basic Research Foundation (2024A1515140058). J. H. also thanks the startup fund from Great Bay University (YJKY230010) and the Guangdong Recruitment Program (2023QN10C724) for support.

Notes and references

1 S. J. Rowan, S. J. Cantrill, G. R. L. Cousins, J. K. M. Sanders and J. F. Stoddart, Dynamic Covalent Chemistry, *Angew. Chem., Int. Ed.*, 2002, **41**, 898–952.
2 Y. Jin, C. Yu, R. J. Denman and W. Zhang, Recent advances in dynamic covalent chemistry, *Chem. Soc. Rev.*, 2013, **42**, 6634–6654.
3 J. Hu, S. K. Gupta, J. Ozdemir and M. H. Beyzavi, Applications of Dynamic Covalent Chemistry Concept toward Tailored Covalent Organic Framework Nanomaterials: A Review, *ACS Appl. Nano Mater.*, 2020, **3**, 6239–6269.
4 Z. Lei, H. Chen, S. Huang, L. J. Wayment, Q. Xu and W. Zhang, New Advances in Covalent Network Polymers via Dynamic Covalent Chemistry, *Chem. Rev.*, 2024, **124**, 7829–7906.
5 A. P. Cote, A. I. Benin, N. W. Ockwig, M. O'Keeffe, A. J. Matzger and O. M. Yaghi, Porous, crystalline, covalent organic frameworks, *Science*, 2005, **310**, 1166–1170.
6 H. M. El-Kaderi, J. R. Hunt, J. L. Mendoza-Cortés, A. P. Côté, R. E. Taylor, M. O'Keeffe and O. M. Yaghi, Designed Synthesis of 3D Covalent Organic Frameworks, *Science*, 2007, **316**, 268–272.
7 X. Feng, X. Ding and D. Jiang, Covalent organic frameworks, *Chem. Soc. Rev.*, 2012, **41**, 6010–6022.
8 S.-Y. Ding and W. Wang, Covalent organic frameworks (COFs): from design to applications, *Chem. Soc. Rev.*, 2013, **42**, 548–568.
9 M. S. Lohse and T. Bein, Covalent Organic Frameworks: Structures, Synthesis, and Applications, *Adv. Funct. Mater.*, 2018, **28**, 1705553.
10 K. Geng, T. He, R. Liu, S. Dalapati, K. T. Tan, Z. Li, S. Tao, Y. Gong, Q. Jiang and D. Jiang, Covalent Organic Frameworks: Design, Synthesis, and Functions, *Chem. Rev.*, 2020, **120**, 8814–8933.
11 J. L. Segura, M. J. Mancheño and F. Zamora, Covalent organic frameworks based on Schiff-base chemistry: synthesis, properties and potential applications, *Chem. Soc. Rev.*, 2016, **45**, 5635–5671.
12 L. Cusin, H. Peng, A. Ciesielski and P. Samorì, Chemical Conversion and Locking of the Imine Linkage: Enhancing the Functionality of Covalent Organic Frameworks, *Angew. Chem., Int. Ed.*, 2021, **60**, 14236–14250.
13 C. Qian, L. Feng, W. L. Teo, J. Liu, W. Zhou, D. Wang and Y. Zhao, Imine and imine-derived linkages in two-dimensional covalent organic frameworks, *Nat. Rev. Chem.*, 2022, **6**, 881–898.
14 Q. Guan, L.-L. Zhou and Y.-B. Dong, Construction of Covalent Organic Frameworks via Multicomponent Reactions, *J. Am. Chem. Soc.*, 2023, **145**, 1475–1496.
15 P. J. Waller, S. J. Lyle, T. M. Osborn Popp, C. S. Diercks, J. A. Reimer and O. M. Yaghi, Chemical Conversion of Linkages in Covalent Organic Frameworks, *J. Am. Chem. Soc.*, 2016, **138**, 15519–15522.
16 H. Liu, J. Chu, Z. Yin, X. Cai, L. Zhuang and H. Deng, Covalent organic frameworks linked by amine bonding for concerted electrochemical reduction of CO2, *Chem*, 2018, **4**, 1696–1709.
17 P. J. Waller, Y. S. AlFaraj, C. S. Diercks, N. N. Jarenwattananon and O. M. Yaghi, Conversion of Imine to Oxazole and Thiazole Linkages in Covalent Organic Frameworks, *J. Am. Chem. Soc.*, 2018, **140**, 9099–9103.
18 J.-M. Seo, H.-J. Noh, H. Y. Jeong and J.-B. Baek, Converting Unstable Imine-Linked Network into Stable Aromatic Benzoxazole-Linked One *via* Post-oxidative Cyclization, *J. Am. Chem. Soc.*, 2019, **141**, 11786–11790.
19 Y. Zhu, D. Huang, W. Wang, G. Liu, C. Ding and Y. Xiang, Sequential Oxidation/Cyclization of Readily Available Imine Linkages to Access Benzoxazole-Linked Covalent Organic Frameworks, *Angew. Chem., Int. Ed.*, 2024, **63**, e202319909.
20 F. Haase, E. Troschke, G. Savasci, T. Banerjee, V. Duppel, S. Dörfler, M. M. J. Grundei, A. M. Burow, C. Ochsenfeld, S. Kaskel and B. V. Lotsch, Topochemical conversion of an imine- into a thiazole-linked covalent organic framework enabling real structure analysis, *Nat. Commun.*, 2018, **9**, 2600.
21 S. Yang, H. Lv, H. Zhong, D. Yuan, X. Wang and R. Wang, Transformation of Covalent Organic Frameworks from N-Acylhydrazone to Oxadiazole Linkages for Smooth Electron Transfer in Photocatalysis, *Angew. Chem., Int. Ed.*, 2022, **61**, e202115655.
22 S. J. Lyle, T. M. Osborn Popp, P. J. Waller, X. Pei, J. A. Reimer and O. M. Yaghi, Multistep Solid-State Organic Synthesis of Carbamate-Linked Covalent Organic Frameworks, *J. Am. Chem. Soc.*, 2019, **141**, 11253–11258.
23 S. Yang, C. Yang, C. Dun, H. Mao, R. S. H. Khoo, L. M. Klivansky, J. A. Reimer, J. J. Urban, J. Zhang and Y. Liu, Covalent Organic Frameworks with Irreversible Linkages via Reductive Cyclization of Imines, *J. Am. Chem. Soc.*, 2022, **144**, 9827–9835.
24 Z.-B. Zhou, H.-H. Sun, Q.-Y. Qi and X. Zhao, Converting Azine Linkage into Highly Stable (Thio)Urea-Based Bicyclic-Fused-Ring Connections in Covalent Organic Frameworks via Criss-Cross [3 + 2] Cycloaddition, *CCS Chem.*, 2024, 1–11.

25 K. Upitak and C. M. Thomas, One-Pot Catalysis: A Privileged Approach for Sustainable Polymers?, *Acc. Chem. Res.*, 2022, **55**, 2168–2179.
26 Y. Hayashi, Pot economy and one-pot synthesis, *Chem. Sci.*, 2016, **7**, 866–880.
27 M. J. Climent, A. Corma and S. Iborra, Heterogeneous Catalysts for the One-Pot Synthesis of Chemicals and Fine Chemicals, *Chem. Rev.*, 2011, **111**, 1072–1133.
28 X.-H. Han, K. Gong, X. Huang, J.-W. Yang, X. Feng, J. Xie and B. Wang, Syntheses of Covalent Organic Frameworks via a One-Pot Suzuki Coupling and Schiff's Base Reaction for C_2H_4/C_3H_6 Separation, *Angew. Chem., Int. Ed.*, 2022, **61**, e202202912.
29 F. J. Uribe-Romo, J. R. Hunt, H. Furukawa, C. Klöck, M. O'Keeffe and O. M. Yaghi, A Crystalline Imine-Linked 3-D Porous Covalent Organic Framework, *J. Am. Chem. Soc.*, 2009, **131**, 4570–4571.
30 M. Matsumoto, R. R. Dasari, W. Ji, C. H. Feriante, T. C. Parker, S. R. Marder and W. R. Dichtel, Rapid, low temperature formation of imine-linked covalent organic frameworks catalyzed by metal triflates, *J. Am. Chem. Soc.*, 2017, **139**, 4999–5002.
31 W. Zhao, Q. Zhu, X. Wu and D. Zhao, The development of catalysts and auxiliaries for the synthesis of covalent organic frameworks, *Chem. Soc. Rev.*, 2024, **53**, 7531–7565.
32 A. Erkkilä, I. Majander and P. M. Pihko, Iminium Catalysis, *Chem. Rev.*, 2007, **107**, 5416–5470.
33 J. Yang, A. Acharjya, M.-Y. Ye, J. Rabeah, S. Li, Z. Kochovski, S. Youk, J. Roeser, J. Grüneberg, C. Penschke, M. Schwarze, T. Wang, Y. Lu, R. van de Krol, M. Oschatz, R. Schomäcker, P. Saalfrank and A. Thomas, Protonated Imine-Linked Covalent Organic Frameworks for Photocatalytic Hydrogen Evolution, *Angew. Chem., Int. Ed.*, 2021, **60**, 19797–19803.
34 Y. Zhao, L. Guo, F. Gándara, Y. Ma, Z. Liu, C. Zhu, H. Lyu, C. A. Trickett, E. A. Kapustin, O. Terasaki and O. M. Yaghi, A Synthetic Route for Crystals of Woven Structures, Uniform Nanocrystals, and Thin Films of Imine Covalent Organic Frameworks, *J. Am. Chem. Soc.*, 2017, **139**, 13166–13172.
35 L. Ascherl, E. W. Evans, J. Gorman, S. Orsborne, D. Bessinger, T. Bein, R. H. Friend and F. Auras, Perylene-Based Covalent Organic Frameworks for Acid Vapor Sensing, *J. Am. Chem. Soc.*, 2019, **141**, 15693–15699.
36 R. Appel, S. Chelli, T. Tokuyasu, K. Troshin and H. Mayr, Electrophilicities of Benzaldehyde-Derived Iminium Ions: Quantification of the Electrophilic Activation of Aldehydes by Iminium Formation, *J. Am. Chem. Soc.*, 2013, **135**, 6579–6587.
37 K. A. Ahrendt, C. J. Borths and D. W. C. MacMillan, New Strategies for Organic Catalysis: The First Highly Enantioselective Organocatalytic Diels−Alder Reaction, *J. Am. Chem. Soc.*, 2000, **122**, 4243–4244.
38 Y.-Q. Zou, F. M. Hörmann and T. Bach, Iminium and enamine catalysis in enantioselective photochemical reactions, *Chem. Soc. Rev.*, 2018, **47**, 278–290.
39 T. Itoh, K. Nagata, A. Kurihara, M. Miyazaki and A. Ohsawa, Reductive amination of aldehydes and ketones by a Hantzsch dihydropyridine using scandium triflate as a catalyst, *Tetrahedron Lett.*, 2002, **43**, 3105–3108.
40 T. Itoh, K. Nagata, M. Miyazaki, H. Ishikawa, A. Kurihara and A. Ohsawa, A selective reductive amination of aldehydes by the use of Hantzsch dihydropyridines as reductant, *Tetrahedron*, 2004, **60**, 6649–6655.
41 C. Zheng and S.-L. You, Transfer hydrogenation with Hantzsch esters and related organic hydride donors, *Chem. Soc. Rev.*, 2012, **41**, 2498–2518.
42 P. Jin, X. Niu, F. Zhang, K. Dong, H. Dai, H. Zhang, W. Wang, H. Chen and X. Chen, Stable and Reusable Light-Responsive Reduced Covalent Organic Framework (COF-300-AR) as a Oxidase-Mimicking Catalyst for GSH Detection in Cell Lysate, *ACS Appl. Mater. Interfaces*, 2020, **12**, 20414–20422.
43 J. Hu, F. Zanca, G. J. McManus, I. A. Riha, H. G. T. Nguyen, W. Shirley, C. G. Borcik, B. J. Wylie, M. Benamara, R. D. van Zee, P. Z. Moghadam and H. Beyzavi, Catalyst-Enabled In Situ Linkage Reduction in Imine Covalent Organic Frameworks, *ACS Appl. Mater. Interfaces*, 2021, **13**, 21740–21747.
44 Q. Zhang, S. Dong, P. Shao, Y. Zhu, Z. Mu, D. Sheng, T. Zhang, X. Jiang, R. Shao, Z. Ren, J. Xie, X. Feng and B. Wang, Covalent organic framework–based porous ionomers for high-performance fuel cells, *Science*, 2022, **378**, 181–186.
45 M. Liu, S. Yang, X. Yang, C.-X. Cui, G. Liu, X. Li, J. He, G. Z. Chen, Q. Xu and G. Zeng, Post-synthetic modification of covalent organic frameworks for CO2 electroreduction, *Nat. Commun.*, 2023, **14**, 3800.
46 Q. Yan, H. Xu, X. Jing, H. Hu, S. Wang, C. Zeng and Y. Gao, Post-synthetic modification of imine linkages of a covalent organic framework for its catalysis application, *RSC Adv.*, 2020, **10**, 17396–17403.
47 L. Grunenberg, G. Savasci, M. W. Terban, V. Duppel, I. Moudrakovski, M. Etter, R. E. Dinnebier, C. Ochsenfeld and B. V. Lotsch, Amine-Linked Covalent Organic Frameworks as a Platform for Postsynthetic Structure Interconversion and Pore-Wall Modification, *J. Am. Chem. Soc.*, 2021, **143**, 3430–3438.
48 H. C. Brown and S. Krishnamurthy, Forty years of hydride reductions, *Tetrahedron*, 1979, **35**, 567–607.
49 M. Zhang, Y. Li, W. Yuan, X. Guo, C. Bai, Y. Zou, H. Long, Y. Qi, S. Li, G. Tao, C. Xia and L. Ma, Construction of Flexible Amine-linked Covalent Organic Frameworks by Catalysis and Reduction of Formic Acid via the Eschweiler–Clarke Reaction, *Angew. Chem., Int. Ed.*, 2021, **60**, 12396–12405.
50 L. Chen, C. Gong, X. Wang, F. Dai, M. Huang, X. Wu, C.-Z. Lu and Y. Peng, Substoichiometric 3D Covalent Organic Frameworks Based on Hexagonal Linkers, *J. Am. Chem. Soc.*, 2021, **143**, 10243–10249.
51 Q. Gao, X. Li, G.-H. Ning, H.-S. Xu, C. Liu, B. Tian, W. Tang and K. P. Loh, Covalent Organic Framework with Frustrated Bonding Network for Enhanced Carbon Dioxide Storage, *Chem. Mater.*, 2018, **30**, 1762–1768.

52 J. Li, G. Chen, C. Chen, Y. Lou, Z. Xing, T. Zhang, C. Gong and Y. Peng, Modulated synthesis of stoichiometric and sub-stoichiometric two-dimensional covalent organic frameworks for enhanced ethylene purification, *Chin. Chem. Lett.*, 2024, **36**, 109760.
53 D. Zhu, Z. Zhang, L. B. Alemany, Y. Li, N. Nnorom, M. Barnes, S. Khalil, M. M. Rahman, P. M. Ajayan and R. Verduzco, *Chem. Mater.*, 2021, **33**, 3394–3400.
54 Y. Liu, Y. Zhu, S. B. Alahakoon and E. Egap, *ACS Mater. Lett.*, 2020, **2**, 1561–1566.
55 D. Zhu and R. Verduzco, *ACS Appl. Mater. Interfaces*, 2020, **12**, 33121–33127.
56 L. Ascherl, E. W. Evans, M. Hennemann, D. Di Nuzzo, A. G. Hufnagel, M. Beetz, R. H. Friend, T. Clark, T. Bein and F. Auras, Solvatochromic covalent organic frameworks, *Nat. Commun.*, 2018, **9**, 3802.
57 Z. Meng, A. Aykanat and K. A. Mirica, Proton Conduction in 2D Aza-Fused Covalent Organic Frameworks, *Chem. Mater.*, 2019, **31**, 819–825.
58 S. Chandra, T. Kundu, S. Kandambeth, R. BabaRao, Y. Marathe, S. M. Kunjir and R. Banerjee, Phosphoric Acid Loaded Azo (−N═N−) Based Covalent Organic Framework for Proton Conduction, *J. Am. Chem. Soc.*, 2014, **136**, 6570–6573.
59 M. Klähn, G. Mathias, C. Kötting, M. Nonella, J. Schlitter, K. Gerwert and P. Tavan, IR Spectra of Phosphate Ions in Aqueous Solution: Predictions of a DFT/MM Approach Compared with Observations, *J. Phys. Chem. A*, 2004, **108**, 6186–6194.
60 Y. A. Fadeeva, I. V. Fedorova, M. A. Krestyaninov and L. P. Safonova, Structural characterization of H3PO3 and H3PO4 acids solutions in DMF: Spectral analysis and CPMD simulation, *J. Mol. Liq.*, 2020, **300**, 112342.
61 R. Sahoo, S. Mondal, S. C. Pal, D. Mukherjee and M. C. Das, Covalent-Organic Frameworks (COFs) as Proton Conductors, *Adv. Energy Mater.*, 2021, **11**, 2102300.
62 Z.-C. Guo, Z.-Q. Shi, X.-Y. Wang, Z.-F. Li and G. Li, Proton conductive covalent organic frameworks, *Coord. Chem. Rev.*, 2020, **422**, 213465.

